NeuroImage **13,** 669–683 (2001)
doi:10.1006/nimg.2000.0714, available online at http://www.idealibrary.com on IDEAL®

Probabilistic Mapping and Volume Measurement of Human Primary Auditory Cortex

J. Rademacher,*,†,[1] P. Morosan,†,‡ T. Schormann,‡ A. Schleicher,‡ C. Werner,*
H.-J. Freund,* and K. Zilles†,‡

**Department of Neurology and ‡C&O Vogt Institute for Brain Research, Heinrich-Heine University, 40225 Düsseldorf; and †Institute of Medicine, Research Center Jülich, Jülich, Germany*

Received June 30, 2000; published online February 2, 2001

Despite their potential utility in clinical and research settings, the range of intra- and interindividual variations in size and location of cytoarchitectonically defined human primary auditory cortex (PAC) is largely unknown. This study demonstrates that gyral patterns and the size and location of PAC vary independently to a considerable degree. Thus, the cytoarchitectonic borders of PAC cannot be reliably inferred from macroscopic—MR visible—anatomy. Given the remarkable topographical variability of architectonic areal borders, standard brain mapping which is made solely on the basis of macroanatomic landmarks may lead to structural–functional mismatch. Consequently, interpretations of individual auditory activity patterns might often be inaccurate. In view of the anatomic discrepancies, we generated probability maps of PAC in which the degree of intersubject overlap in each stereotaxic position was quantified. These maps show that the location of PAC in Talairach space differs considerably between hemispheres and individuals. In contrast to earlier cytoarchitectonic work which is based in most cases on studies of single brains, our systematic approach provides extensive microanatomic data as a reference system for studies of human auditory function. © 2001 Academic Press

Key Words: **human cerebral cortex; auditory cortex; cytoarchitecture; image analysis; brain mapping.**

INTRODUCTION

Topography and size of human primary auditory cortex (PAC) vary between the classical cytoarchitectonic parcellations as well as between individual brains (Brodmann, 1909; von Economo and Koskinas, 1925; von Economo and Horn, 1930; Braak, 1980; Galaburda and Sanides, 1980; Rademacher *et al.*, 1993; Rivier and Clarke, 1997; Clarke and Rivier, 1998). It is not known to which degree divergent measures of auditory functions reflect either anatomic variability or individual differences in cognitive processes. To date, knowledge about the precise degree of biological variability in shape, extent, and localization of borders has been quite limited, because time-consuming cytoarchitectonic analysis has typically been restricted to only a single or too few brains. The Brodmann map provides a schematic concept of temporal lobe architecture and of area 41, which represents PAC in mammalian brains (Brodmann, 1909). Individual variations in the course of the major brain gyri and sulci have not been considered (Eberstaller, 1890; Cunningham, 1892; Ono *et al.*, 1990). Unfortunately, high-resolution MR imaging does not allow *in vivo* detection of the cytoarchitectonic features of PAC.

The authors of the classical anatomical brain maps assume a lack of variability in the entire population, including interhemispheric symmetry and interindividual equality. However, today we are aware of the fact that there can be considerable anatomic variability in the position, size, and shape of cortical structures. The gyral pattern especially of the superior temporal region which contains the auditory cortex is highly variable. Up to five transverse gyri (Campain and Minckler, 1976) and marked interhemispheric asymmetries (Geschwind and Levitsky, 1968; Penhune *et al.*, 1996; Pfeifer, 1920; von Economo and Horn, 1930) have been described. In an earlier cytoarchitectonic study by one of the authors, Brodmann area 41 was found to be larger on the left side in 6 of 10 brains (Rademacher *et al.*, 1993). Furthermore, the issue of how architectonic field borders relate to primary or secondary brain sulci is frequently neglected in both structural and functional neuroimaging studies of PAC. It has been hypothesized that the folding occurs at the border between two architectonically distinct cortical areas (Sanides, 1962). Hence, the location of the transverse temporal sulci (Leonard *et al.*, 1998)

[1] To whom correspondence and reprint requests should be addressed at the Department of Neurology, Heinrich-Heine-University, Moorenstrasse 5, 40225 Düsseldorf, Germany. Fax: +49-211-8112336. E-mail: j.rademacher@fz-juelich.de.

1053-8119/01 $35.00

may mark the borders between specific architectonic areas.

The interest in mapping cerebral gyri and sulci stems from issues of functional localization. *In vivo* human cognitive neuroanatomy is based on the identification of the anatomical substrate of human behavioral variation (Rademacher *et al.*, 1992). In this context, planum temporale asymmetry has motivated many observers to study the auditory cortex, taking Heschl's gyrus (HG) and the planum as its macroanatomic markers. Duplications of HG are increased in families with learning disabilities (Leonard *et al.*, 1993) and planum temporale patterns are related to handedness, absolute pitch, and musical ability (Witelson and Kigar, 1988; Steinmetz *et al.*, 1991; Schlaug *et al.*, 1995). Thus, the sizes of HG and the planum temporale have been interpreted as indicators of the efficiency and complexity of auditory and language processing. Although it has become conventional to refer to HG as the site of PAC and to the planum temporale as the site of auditory association cortex, one may challenge the concept of tight associations between micro- and macroanatomic parcellations. The finding of striking variations in the sulcal landmarks of HG has demonstrated that anatomic variability poses serious obstacles to the attempt to map behavioral function onto the brain (Leonard *et al.*, 1998).

Given the lack of information on architectonic variability, most observers using functional imaging of auditory processing (Romani *et al.*, 1982; Lauter *et al.*, 1985; Pantev *et al.*, 1988, 1990; Liegeois-Chauvel *et al.*, 1991) relate their findings to a standardized coordinate system (Talairach and Tournoux, 1988) or to gross morphological landmarks such as HG (Penhune *et al.*, 1996). However, variability of temporal lobe anatomy may represent important pitfalls to these approaches (Steinmetz *et al.*, 1990a; Rademacher *et al.*, 1993), and discrepancies between functional maps may be related to the variability in size and geometry of the temporal cortex. These limitations may explain in part why there is still a debate about the localization and asymmetries of human auditory responses (Hashimoto *et al.*, 1995; Ohtomo *et al.*, 1998; Zouridakis *et al.*, 1998). Clarification requires an overlay of cytoarchitectonic areas with functionally defined areas in a common reference system. The problem of individual variability adds a distortion correction requirement that can be implemented by the use of a three-dimensional (3-D) probabilistic mapping strategy which is based on an anatomical atlas system (Roland *et al.*, 1994; Mazziotta *et al.*, 1995; Zilles *et al.*, 1995). Its usefulness has been demonstrated recently for the motor (Geyer *et al.*, 1996), somatosensory (Geyer *et al.*, 1999), and visual cortex (Amunts *et al.*, 2000) as well as for Broca's area (Amunts *et al.*, 1999). These studies described individual volume differences of distinct cytoarchitectonic areas of up to a factor of 10 across subjects.

In analogy, if we wish to estimate the probability of auditory response generation at a certain point in PAC, we have to know not only the local status of neuronal response characteristics, but also the relationship between them and the spatial extent of PAC. Similarily, if we wish to facilitate the development of a sound basis for *in vivo* cognitive neuroanatomy, we need to know more about the homologies of MR visible macroanatomic markers across individual hemispheres and brains. For the auditory cortex, improved mapping strategies and more architectonic data are needed to accommodate for structural variability. In our companion article (P. Morosan *et al.*), we describe the application of a recently developed cytoarchitectonic mapping technique which is based on quantitative gray level index (GLI) measures and an *in vivo* 3-D reference brain. PAC (i.e., Te1) has been found to consist of three cytoarchitectonic areas (Te1.1, Te1.0, Te1.2) along the mediolateral axis of Brodmann area 41. For the present cytoarchitectonic study, which is the largest ever performed on the auditory cortex, we analyzed the precise topographical patterns of area Te1 (i.e., total PAC) in 27 human postmortem brains. The goals of the present study were (i) the description of the range/variability of anatomical phenotypes regarding the shape, size, and extent of area Te1 bilaterally; (ii) the analysis of the relationship between sulcal landmarks and architectonic borders; and (iii) the 3-D reconstruction and mapping of area Te1 to a standard brain in order to compare our data with the results of previous anatomical or functional studies.

MATERIALS AND METHODS

Subjects

Twenty-seven adult human postmortem brains were obtained from the body donor program of the Anatomical Institute of the University of Düsseldorf in accordance with the legal requirements. None of the subjects had a history of neurological or psychiatric disease. The subjects consisted of 14 females and 13 males ages 37 to 85 years. None of the brains was included in a previous study which was performed by one of the authors (Rademacher *et al.*, 1993). Handedness of the subjects was unknown, but it can be assumed that—similar to the incidence of the general population—approximately 90% of our cases will have been right-handed (Gilbert and Wysocki, 1992).

Identification of Major Landmarks

A reliable definition of the primary gyri and sulci (frequency 100%; Ono *et al.*, 1990) on the superior temporal plane is mandatory for brain mapping studies of human auditory cortex. Figure 1 shows the macroanatomic topography. In the depth of the Sylvian

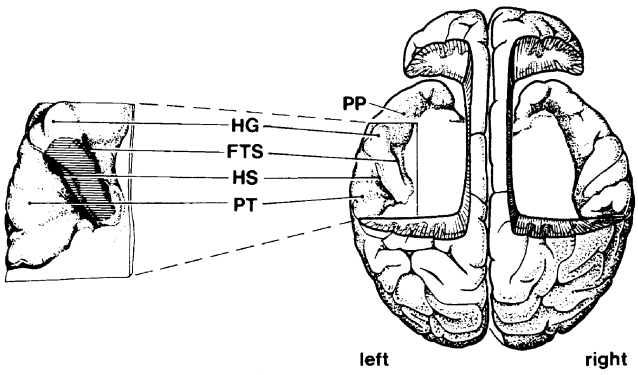

FIG. 1. Anatomic definition of Heschl's gyrus (HG). The exposed surface of the superior temporal plane shows the oblique course of HG bilaterally (view from above; anterior is at the top). HG is located between the planum polare (PP) and the planum temporale (PT). As shown for the left hemisphere, the anteromedial border of HG is defined by the first transverse sulcus (FTS) and its posterior border is defined by Heschl's sulcus (HS). On the left side the reconstructed map of cytoarchitectonic area Te1 is visualized (hatching occupying HG). In our example, the right-sided superior temporal plane shows two transverse gyri. This indicates that the definition of HG by macroanatomic criteria alone may remain equivocal.

fissure, HG is the rostralmost transverse gyrus and can be identified by its prominent size and characteristic shape (Steinmetz *et al.*, 1989). Its oblique course extends from the retroinsular region medially to the rim of the first temporal gyrus laterally. Heschl's sulcus is located between HG anteriorly and the planum temporale posteriorly. Additional transverse gyri may cover the planum temporale (Fig. 1, right hemisphere). The first transverse sulcus is located between the planum polare anteriorly and HG posteriorly. Additional transverse gyri on the planum polare have not been described. The intermediate transverse sulcus, present in up to 50% of hemispheres (Leonard *et al.*, 1998), indents HG along its long axis and subdivides it—completely or incompletely—into anterior and posterior portions termed "duplications" (Penhune *et al.*, 1996). The topographical variations of gyri and sulci and the total number of transverse gyri on the superior temporal surface in each hemisphere were determined.

MR Imaging and Histological Processing of Postmortem Brains

All 27 postmortem brains were fixed in 4% formalin or in Bodian's solution with a postmortem delay between 8 and 24 h. Ten of 27 brains were studied with MR imaging prior to histological processing as described in the companion article (P. Morosan *et al.*). In brief, the immersion-fixed brains were scanned (Siemens Magnetom 1.5 T) in a water-filled vacuum globe in order to reduce image distortions by trapped air bubbles. The applied 3-D FLASH fast gradient echo sequence had a resulting voxel size of $1 \times 1 \times 1.17$ mm, which provided sufficient resolution for 3-D computer reconstructions. All brains were dehydrated in graded series of alcohol, embedded in paraffin, and serially sectioned (20-μm-thick sections). Every 15th section was silver stained for cell bodies (Merker, 1983) and every 60th section was used for quantitative volumetric analysis and 3-D reconstruction of area Te1. Ten brains were analyzed in whole brain coronal serial sections and 17 brains were analyzed in blocks cut perpendicular to the main axis of HG thereby avoiding cutting artifacts caused by oblique sections.

Cytoarchitectonic Analysis

The cytoarchitecture of every 60th section of the paraffin-embedded brains was analyzed under low magnification through a stereomicroscope guided by the criteria neuronal packing density, cell size, arrangement, and staining intensity as described in the companion article (P. Morosan *et al.*). Area Te1 (i.e., Brodmann area 41) was recognized in all 54 hemispheres by its general parvocellularity, the high packing density of neurons, and the prominent width of layer IV (Rademacher *et al.*, 1993). It represents the auditory koniocortex including areas Te1.2, Te1.0, and Te1.1, surrounded by less granular auditory parakoniocortex (Galaburda and Sanides, 1980). The borders and surface extent of area Te1 were mapped to the glass-covered sections onto their individual sulcal patterns in all 54 hemispheres. These borders were validated in 20 hemispheres by automated GLI measurements as described in the companion article (P. Morosan *et al.*) and, more extensively, by Schleicher *et al.* (1999). The observer-independent areal borders of area Te1, defined by significant changes in the shape of the GLI curves, were in good agreement with the areal borders as defined by visual inspection and standard cytoarchitectonic analysis. This finding was taken as a proof of the reliability of the classical approach for PAC border definition by visual inspection. We have analyzed total PAC—and not its subparcellations—in order to provide data that can be related to previous structural and functional studies. Further parcellation of PAC has led to a variety of maps by different authors in which homologies of putative architectonic areas are difficult to ascertain (von Economo and Koskinas, 1925; von Economo and Horn, 1930; Hopf, 1954; Braak, 1980; Galaburda and Sanides, 1980; Rivier and Clarke, 1997; Clarke and Rivier, 1998).

Mapping Strategies

Individual Maps of Area Te1

Since gyral and sulcal landmarks are reliably visualized with *in vivo* MR imaging, it is relevant to studies of brain–behavior relationships to relate architectonic findings to macroanatomic landmarks. In this context, individual cytoarchitectonic maps represent the stan-

dard approach to visualize microanatomic parcellation (von Economo and Horn, 1930; Braak, 1980; Galaburda and Sanides, 1980; Rademacher *et al.*, 1993; Rivier and Clarke, 1997; Clarke and Rivier, 1998). In the present study, the location of area Te1 in each hemisphere of the total series of 54 hemispheres was mapped to surface and coronal views of the respective individual supratemporal plane. The surface views were based on photographs of the intact and exposed supratemporal plane after section of the frontoparietal operculum. The visible sulcal landmarks were used for a proportional mapping of cytoarchitectonic area Te1 onto the transverse gyri. Slice thickness, distance from slice to slice, and linear shrinkage factors were used as parameters for creating a proportional enlargement of the shrunken area onto the photograph of the normal-sized brain. We refrained from providing a metric for the maps, because the classic 2-D line drawings of 3-D surface topography cannot be a true representation of the real distances.

Probabilistic Maps of Area Te1

In 20 hemispheres of the series, area Te1 was mapped to a computerized brain atlas, which is represented by an *in vivo*-acquired 3-D MR data set of an individual brain. The procedure has already been described in detail elsewhere (Roland *et al.*, 1994; Zilles *et al.*, 1995; Amunts *et al.*, 1999, 2000; Geyer *et al.*, 1999). Mapping of the labeled volumes of area Te1 onto the reference brain results in a 3-D map of the probability that area Te1 will be found at a given voxel location in stereotaxic space. For this purpose, all coronal histological sections of each brain were digitized (KS400, Zeiss), then matched to the corresponding 3-D MR volume, and ultimately warped to the computerized reference brain by means of an affine matching procedure (i.e., rotation, translation, scaling) (Schormann *et al.*, 1997; Schormann and Zilles, 1998). Hence, area Te1 maintained its individual shape, and interhemispheric topographical asymmetries could be analyzed. Consecutively, we generated an atlas-based 3-D probability map representing location and extent of area Te1 in 10 left and 10 right hemispheres. Probabilistic contour maps can then be used to localize a region of interest within PAC for a given range of probability.

Talairach Atlas

The spatially normalized brains—and area Te1—were transferred to the Talairach space (Talairach and Tournoux, 1988) by a simple coordinate transformation in order to relate our cytoarchitectonic findings to this normative stereotaxic database and to earlier studies of structure and function in the human auditory cortex. The extent of area Te1 in the sagittal, coronal, and horizontal planes was calculated in Talairach coordinates. In Talairach space, the *x* axis defines the mediolateral direction, with negative values indicating the left hemisphere. The *y* axis defines the anterior–posterior direction, with positive values anterior to the orthogonal plane through the anterior commissure and negative values posterior to this landmark. The *z* axis is defined by the horizontal plane which passes through anterior and posterior commissures (AC–PC line), with positive values superior to it and negative values inferior to it. The bounding box for area Te1 (i.e., maximal extent in the three standard Talairach planes (Penhune *et al.*, 1996)) was measured in each brain and averaged across 10 brains. The results were compared to those of other brain mapping studies. Interhemispheric comparisons for minimum and maximum *x*, *y*, and *z* values of Te1 were performed as well using paired *t* tests for dependent samples (Bonferroni corrected).

Measurements of Area Te1 and HG

On every 60th histological section the extent of area Te1 and HG (mm^2) was measured separately for each hemisphere with an electronic planimeter. The individual volumes of area Te1 and HG (mm^3) were calculated by adding the single slice measurements multiplied by slice thickness and distance. The borders of HG used were: (i) the depth of the first transverse sulcus anteromedially, (ii) the depth of Heschl's sulcus posteriorly, and (iii) the lateral hemispheric margin laterally (Rademacher *et al.*, 1992). The intermediate sulcus was not taken as a border because of its inconsistency (Ono *et al.*, 1990; Leonard *et al.*, 1998). When two or more transverse gyri originated separately from the retroinsular region, only the most anterior gyrus was taken as HG, regardless of side (Steinmetz *et al.*, 1989). In order to correct our measurements for individual brain shrinkage during histological processing, we calculated a mean shrinkage factor from 10 brains [shrinkage factor (sf) = histological brain volume/fresh brain volume; mean sf = 0.496]. Volumetric data which represent the true *in vivo* size of HG and PAC were then generated from the histological measures according to the formula: fresh volume = histological volume x 1/shrinkage factor. For a better understanding of the relative size of PAC, we also calculated proportional dimensionless values (PAC/HG) from the data. Interhemispheric asymmetry of area Te1 (and HG) was defined as any side difference which is larger than 10% and its degree was determined as the coefficient $\delta Te1 = (V_R - V_L)/(0.5(V_R + V_L))$, which corrects for total (R, right and L, left) Te1 size (*V*, volume) (Galaburda *et al.*, 1987; Rademacher *et al.*, 1993). Negative values of δTe1 indicate leftward asymmetries and positive values indicate rightward asymmetries. The volumes of area Te1 and HG were compared between hemispheres and sexes (two-way ANOVA with repeated-measurements design; $\alpha < 0.05$). Mean vol-

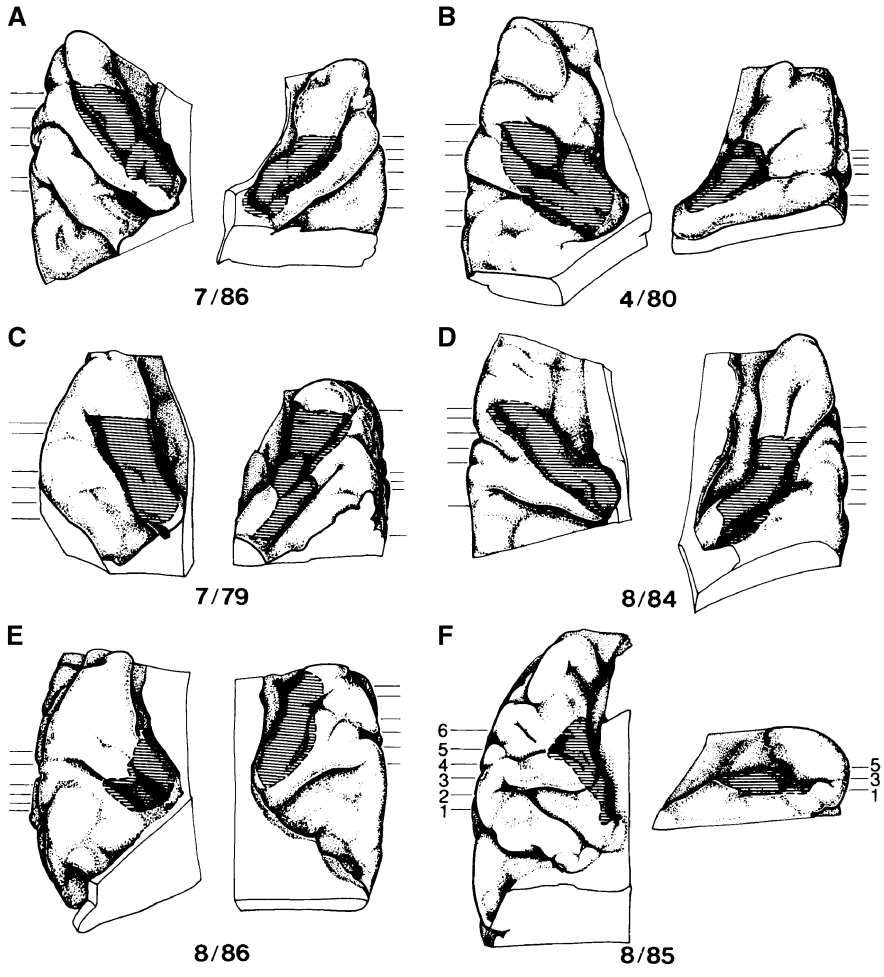

FIG. 2. Topography of area Te1. Drawings from photographs of the superior temporal plane showing reconstructed maps of area Te1 (hatching occupying varying proportions of Heschl's gyrus) in six left and right hemispheres representative of our sample (view from above; anterior is at the top, the temporal pole is not shown, left is on the left, numbers represent brain codes). Coronal cuts from the same brains are shown in Fig. 3 (see cross reference marks in Figs. 2F and 3F).

umes of both regions of interest were calculated by averaging individual volumes. For the analysis of the association between HG volumes and Te1 volumes, Pearson correlation coefficients were calculated. Left–right comparisons of volumes were performed by a paired (left vs right hemisphere) t test ($\alpha < 0.05$).

RESULTS

Gyral and Sulcal Variations

Variations in the number of transverse gyri included a single transverse gyrus in 38 of 54 hemispheres (70%), two transverse gyri in 13 of 54 hemispheres (24%), and three transverse gyri in 3 of 54 hemispheres (6%). The first transverse sulcus and Heschl's sulcus were found in all hemispheres. An intermediate transverse sulcus was present in 22 of 54 hemispheres (41%). There were no significant side differences in the number of gyri or sulci. Examples of geometric variations of gyri and sulci are depicted in Figs. 2 and 3.

Mapping Strategies

Individual Maps of Area Te1

Cytoarchitectonic criteria, established for the preceding companion study of 20 hemispheres, also proved valid for the whole series of 54 hemispheres. In each case, the largest portion of area Te1 was localized on HG. At the medial (retroinsular) origin of HG, a narrow strip of cortex contained hypocellular prokoniocortex with dominating infragranular layers. Laterally and on the adjacent superior temporal plane, belt areas of auditory association cortices could be distinguished (Galaburda and Sanides, 1980). Individual cytoarchitectonic maps showing the surface topography of area Te1 bilaterally are depicted in Fig. 2 (dorsal view; $n = 8$) and Fig. 3 (coronal sections; $n = 6$). In our series,

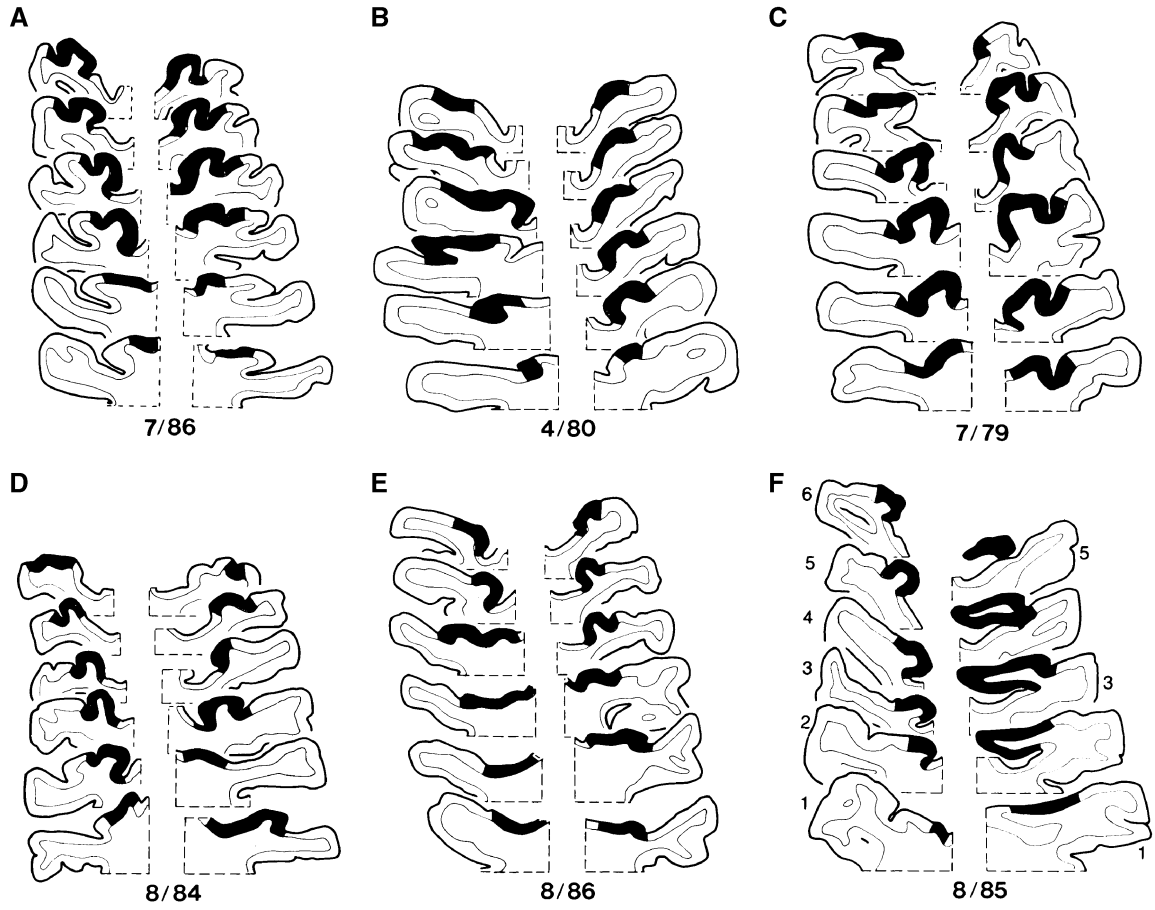

FIG. 3. Topography of area Te1. Camera lucida drawings of six representative coronal cuts taken from different levels of the superior temporal plane showing area Te1 (hatching) in six left and right hemispheres (from the same brains as in Fig. 2, see cross reference marks in Figs. 2F and 3F). The view is from anterior; caudal is at the top, left is on the left, and numbers represent the individual brain codes.

area Te1 does not extend to the lateral brain convexity but portions of area Te1 may reach the planum polare or planum temporale to varying degrees. There are no sulcal landmarks for the medial (prokoniocortex) and lateral (association cortex) borders of area Te1. The lateral flattening of HG is not a reliable macroanatomic sign to detect the field boundary. Anteriorly, the first temporal transverse sulcus represents only an approximate landmark for the border of area Te1 which does not coincide with this sulcus along its total mediolateral extent (Figs. 2 and 3). Similarily, Heschl's sulcus may be taken as the approximate posterior border of area Te1, but here again the overlap is far from perfect. In addition, there is great variability among the inconsistent secondary sulci. The intermediate transverse sulcus, present in less than half of our sample, represents an approximate posterior border of area Te1 in 14 hemispheres (64%) (for example, Fig. 2A) while it does not do so in 8 hemispheres (36%) (for example, Fig. 2B). Smaller tertiary sulci complicate the cortical surface patterns and do not follow consistent patterns. For variations in shape, see for example the curved pattern of area Te1 in Fig. 2C (right side) and the unusual topography of HG and area Te1 in Fig. 2F. The representations of area Te1 in the coronal plane provide further details about the relationship between the course of the sulci and the localization of areal borders (Fig. 3). The cytoarchitectonic borders may be located in a sulcal fundus or they may be found on one or the other wall of two neighboring gyri. In general, right-sided area Te1 does not appear to be the mirror image of (contralateral) left-sided area Te1.

Probabilistic Maps of Area Te1

Figure 4 presents color-coded maps of area Te1 for the regions of identical probability in standardized space from 10% (dark blue) to 100% (dark red) in steps of 10%. Three standard planes are depicted (coronal, axial, and sagittal planes) with cross-reference marks superimposed to visualize the principle and utility of multiple (orthogonal) views in the computerized 3-D reference system. The axial plane shows that the location of area Te1 on the right side is shifted anteriorly,

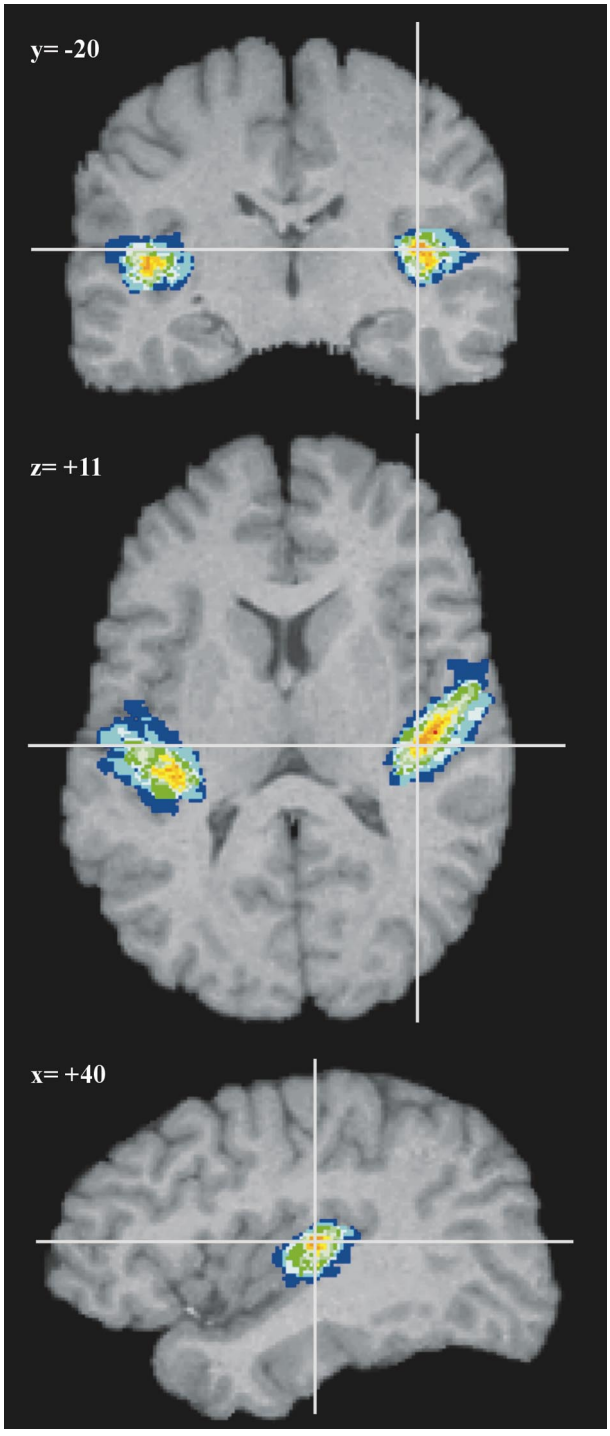

FIG. 4. Probability maps of area Te1. As an example, coronal, axial, and sagittal slices through the computerized reference brain (MR images) are shown (*x*, *y*, and *z* values are Talairach planes). Cross-reference marks are visualized to indicate the multiple (orthogonal) views. The probability maps of cytoarchitectonically defined area Te1 from 10 brains have been superimposed. Color code: increasing probabilities from dark blue (10% overlap) to dark red (100% overlap).

compared to its homologue on the left side. The axial plane also indicates that area Te1 is shifted laterally on the right side (see below, for quantitative data).

While the topography of area Te1 varies, the overall variability does not differ markedly between the hemispheres. In Fig. 5, the probability maps for 10 horizontal slices are overlaid on a grid in standardized space at 2-mm intervals. These maps can be used as an atlas to localize area Te1 for a given range of probability. For example, a significant focus of activation in a patient with acoustic hallucinations was observed in the left hemisphere at $x = 47$, $y = -15$, and $z = 12$ (Dierks *et al.*, 1999); it would be found in the $z = 12$ map of area Te1 within the 60% probability range.

In the present study, significant side differences were observed for the location of area Te1 in the sagittal and coronal planes (Table 1). Compared to the left side, right-sided area Te1 is shifted more than 5 mm laterally. In the coronal plane, the right-sided rostral and caudal borders of area Te1 are shifted ~7 mm anteriorly. The centroids of area Te1 ($n = 10$ brains) show the largest side differences in the coronal plane (left side, $x = -42$, $y = -21$, $z = +7$; right side, $x = +46$, $y = -13$, $z = +8$). Maximum individual asymmetries (i.e., the maximum difference between any pair of hemispheres) ranged from 9 mm in the sagittal and axial planes to 13 mm in the coronal plane.

Talairach Atlas

Linear scaling and transformation of area Te1 to the standard brain permits direct comparison of our architectonic data with the Talairach atlas and the results from other studies. The maximal areal extent in stereotaxic space was outlined separately for both sides by defining the bounding box which contains the total volume of area Te1 from 10 brains. The resulting *x*, *y*, and *z* coordinates define the maximal topographic variability of area Te1. The average location of PAC as defined by cytoarchitectonic area Te1 differs in all dimensions from the location of PAC as defined in the Talairach atlas (Table 1). In the *x* dimension, the lateral border is shifted medially by ~4 mm (right side) to ~10 mm (left side). The medial border is shifted laterally by ~3 mm on the right side and medially by ~2 mm on the left side. The anterior border (*y* dimension) of the right PAC, which was assumed to be the mirror equivalent of the left PAC by Talairach and Tournoux (1988), is shifted rostrally by ~7 mm. Also the posterior border is shifted rostrally, by ~11 mm on the right and ~4 mm on the left side. In the axial plane (*z* dimension), the inferior borders are shifted ventrally by ~4 mm (right side) to ~6 mm (left side). The maximum differences between the stereotaxic coordinates of area Te1 in individual hemispheres and HG in the Talairach atlas (i.e., the highest degree of mismatch) were 16 mm in the sagittal plane, 18 mm in the coronal plane, and 14 mm in the axial plane. To facilitate comparison, we used the same Talairach coordinates for PAC as did previous authors (Penhune *et al.*, 1996).

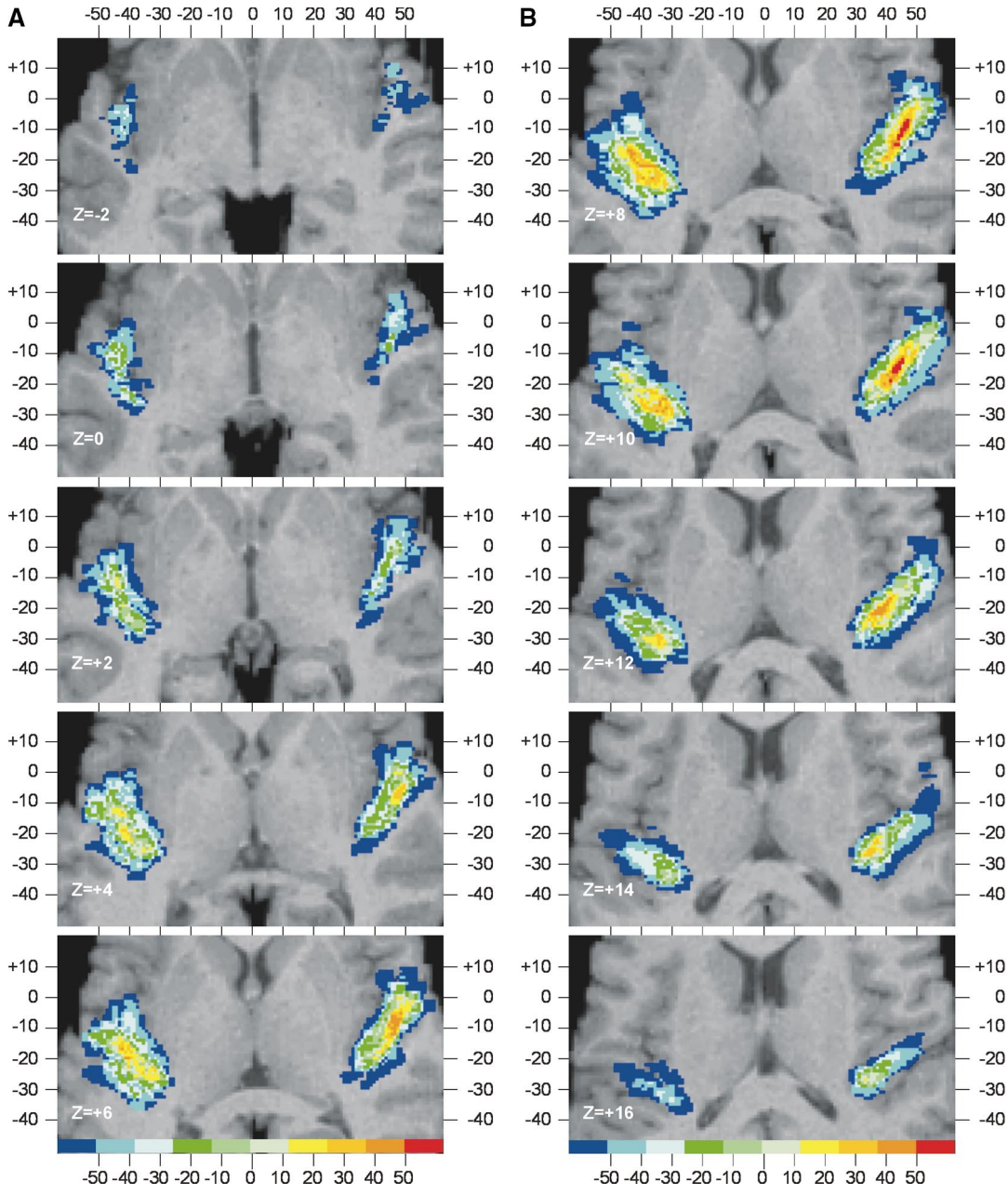

FIG. 5. Atlas of area Te1. Probability maps of area Te1 at 10% steps in 10 horizontal slices overlaid on a grid in standardized space (*z* separation = 2 mm; range, *z* = 0–16). In all slices, the outer contour (dark blue) represents 10% overlap. Grid scale in mm (1:2); *x* coordinates labeled horizontally, *y* coordinates labeled vertically. The left hemisphere is on the left side. (A) Horizontal slices from $z = -2$ to +6. (B) Horizontal slices from $z = +8$ to +16.

It is important to note, however, that the Talairach atlas provides only crude information about the extent of Brodmann area 41 and that the extent of HG as visualized in the atlas is smaller ($x = 29$ *to* 55, $y = -16$ to -35, $z = 8$ to 16) than assumed by Penhune and co-workers.

The average location of PAC as defined by cytoarchitectonic area Te1 also differs from the average location of PAC as defined by HG in the study of Penhune *et al.* (1996) (Table 1). For precision, we used only the high-resolution data from that study. The largest difference was found for the lateral borders of PAC. It is shifted medially by ~10 mm on the left side and ~6 mm on the right side. The medial border is shifted medially by ~2 (right) to ~5 mm (left). The anterior border of PAC is shifted rostrally by ~1 (left) to ~3 mm (right) and the posterior border is shifted caudally by ~2 mm (left side only). In the axial plane, there is an ~3-mm ventral shift of superior and inferior borders on the left side only. The maximum differences between the stereo-

TABLE 1

Mean Values for Minimum and Maximum *x*, *y*, and *z* Values of Primary Auditory Cortex in Stereotaxic Coordinates of the Talairach Atlas

		x dimension (sagittal plane)		*y* dimension (coronal plane)		*z* dimension (axial plane)	
Authors	Side	Min	Max	Min	Max	Min	Max
Present study[1]	Left	−26.9 ± 2.1[a]	50.8 ± 3.5[a]	−34.5 ± 3.2[a]	−3.6 ± 4.3[a]	−1.9 ± 4.0	14.7 ± 2.1
	Right	32.3 ± 1.9[a]	56.7 ± 3.1[a]	−27.9 ± 3.8[a]	3.2 ± 5.3[a]	−0.1 ± 3.8	16.0 ± 2.1
Penhune *et al.* (1996)[2]	Left	−31.5 ± 2.2[a]	60.4 ± 4.2	−32.8 ± 3.2[a]	−4.7 ± 5.2[a]	1.1 ± 2.8	17.7 ± 2.3[a]
	Right	34.0 ± 2.8[a]	62.4 ± 4.5	−28.7 ± 3.4[a]	0.1 ± 5.8[a]	0.3 ± 4.1	16.0 ± 2.8[a]
Talairach and Tournoux (1988)[2]	Left	−29	−61	−35	−8	4	16
	Right	29	61	−35	−8	4	16

Note. 1, cytoarchitectonic area Tel 1; 2, Heschl's gyrus. In the *x* dimension statistical analysis was performed on absolute min/max values.
[a] Significant difference ($p < 0.05$) between the hemispheres.

taxic coordinates of area Te1 in individual hemispheres and the spatial location of HG in the study of Penhune *et al.* (1996) are ~15 mm in the sagittal plane, ~10 mm in the coronal plane, and ~11 mm in the axial plane. In these cases, area Te1 was located more medially, more rostrally, and more ventrally than HG.

Measurements of Area Te1 and HG

Table 2 shows the individual volumes, means, and standard deviations of left ($n = 27$) and right ($n = 27$) areas Te1 and HG. The respective volumes vary within a wide range both interhemispherically and interindi-

TABLE 2

Left and Right Volumes and Asymmetry Coefficients of Area Te1 and Heschl's Gyrus

	Area Te1 volume (mm^3)			Heschl gyrus volume (mm^3)		
Brain	Left	Right	δTe1	Left	Right	δHG
1	1721	2132	0.21 R	3198	3432	0.07 S
2	1662	2178	0.27 R	2369	2978	0.23 R
3	1313	1399	0.06 S	2718	3067	0.12 R
4	2092	828	−0.87 L	4811	4176	−0.14 L
5	1577	1242	−0.24 L	4067	2414	−0.51 L
6	1086	1147	0.05 S	2942	3155	0.07 S
7	830	1071	0.25 R	4915	3090	−0.46 L
8	2681	2173	−0.21 L	3392	3473	0.02 S
9	1198	926	−0.26 L	3034	3198	0.05 S
10	2440	1488	−0.48 L	4409	2525	−0.54 L
11	1327	1803	0.30 R	4732	5212	0.10 S
12	1140	599	−0.62 L	7217	1924	−1.16 L
13	1709	1845	0.08 S	2105	2224	0.05 S
14	1564	1224	−0.24 L	2026	1686	−0.18 L
15	1412	960	−0.38 L	2726	2747	0.01 S
16	1559	787	−0.66 L	2236	1429	−0.44 L
17	1665	1630	−0.02 S	2371	2125	−0.11 L
18	1698	1757	0.03 S	2742	2416	−0.13 L
19	1252	1351	0.08 S	3302	2218	−0.39 L
20	1069	1386	0.26 R	2703	3574	0.28 R
21	1525	2059	0.30 R	4183	3465	−0.19 L
22	2797	2366	−0.17 L	3762	3020	−0.22 L
23	2485	1678	−0.39 L	3742	5282	0.34 R
24	1292	1421	0.09 S	1965	2534	0.25 R
25	2336	2510	0.07 S	2529	3010	0.17 R
26	1500	2787	0.60 R	2579	4415	0.53 R
27	2520	1926	−0.27 L	5311	3896	−0.31 L
Mean	1683	1581	−0.08	3411	3062	−0.09
SD	538	564	0.34	1231	956	0.35

Note. L, δTe1 left > right; R, δTe1 right > left; S, symmetry.

vidually. Analysis of variance for repeated measures (regions: area Te1, HG) showed a significant effect of region ($F(1,25) = 76.2$; $P < 0.0001$) that was unrelated to the sex of the subject ($F(1,25) = 0.25$; $P > 0.5$). In each hemisphere, the individual volumes of HG were larger than the ipsilateral volumes of area Te1 (Table 2). The relative size of area Te1, expressed as a proportion of the total individual volume of ipsilateral HG, ranges from 16 to 92% (mean, 54%). On the left side it varies between 16 and 92% (mean ± SD; 54 ± 20%) and on the right side it varies between 20 and 83% (mean ± SD, 54 ± 18%). The volume of area Te1 does not correlate with the volume of HG.

The asymmetry indices δTe1 and δHG were calculated for each subject and the results are summarized in Table 2. Leftward asymmetries result in negative values, rightward asymmetries result in positive values. The individual asymmetry measures show no clear pattern. A leftward asymmetry of area Te1 is present in 12 of 27 brains (44%), while a rightward asymmetry is present in 7 of 27 brains (26%). Eight brains (30%) are symmetric for the size of area Te1. Side differences of area Te1 and HG were not statistically significant.

DISCUSSION

The cytoarchitecture of human PAC has been studied since the beginning of the past century (Brodmann, 1909; von Economo and Koskinas, 1925; von Economo and Horn, 1930). Advances in functional imaging of auditory processing have promoted intensive microanatomic research in the past decade (Rademacher *et al.,* 1993; Rivier and Clarke, 1997; Clarke and Rivier, 1998). While modern imaging techniques have further increased our understanding of the functional organization of auditory cortex, they also set new standards for precise and reliable anatomical maps as a prerequisite for the topographical interpretation of activation clusters. Visualization is an essential element in data analysis to answer the question whether a distinct auditory activation is located within a specific architectonic area. Appropriate methods of presentation should convey information about the correlation between MR visible landmarks and architectonic borders as well as information about the characteristic spatial extent of an architectonic area in the population. Our results show how the first objective can be achieved by individual landmark-based anatomical maps (Figs. 2 and 3) while the second objective requires mapping of the individual data to a spatial reference system (Figs. 4 and 5). The use of quantitative volumetric techniques complements our approach (Tables 1 and 2).

It is well known that Brodmann area 41 is located in the depth of the Sylvian fissure, but its extent on HG and the neighboring transverse gyri varies between hemispheres and brains (Rademacher *et al.,* 1993). Such variation may depend on the architectonic method used to define PAC. Compared to the pigment-architectonically defined granular core area that is reported exclusively on the medial half of HG (Braak, 1978), cytoarchitectonically defined PAC extends more laterally and covers about two-thirds of HG (von Economo and Koskinas, 1925). We applied established and novel quantitative brain mapping strategies to the cytoarchitectonic analysis of human PAC. Our results demonstrate that there is considerable intra- and interindividual variability in the localization and extent of human PAC. The location of area Te1 can be defined by MR visible anatomic landmarks, but with striking differences in the degree of confidence regarding its borders. Area Te1 always covers portions of HG and is surrounded by belt areas of prokoniocortex or auditory association cortex (Galaburda and Sanides, 1980; Rademacher *et al.,* 1993). However, there is no consistent and reliable association between gyri and sulci and cytoarchitectonic borders. The precise location and absolute size of area Te1 cannot be reliably inferred from the macroanatomic landmarks. HG may serve only as a structural marker of the location of PAC. Especially the mediolateral and anteroposterior extent of area Te1 do not covary with macroanatomy. A similar lack of a precise correspondence between gyral and sulcal landmarks and a distinct cytoarchitectonic area has been reported for the medial occipital lobe and Brodmann area 17, i.e., primary visual cortex (Amunts *et al.,* 2000). It was concluded that it is not possible to make valid predictions about the location of cytoarchitectonic areas and especially their borders, based on the macroscopic surface anatomy alone. We suggest that sufficient insight into the range of topographical variations depends on the (complementary) description of individual cytoarchitectonic phenotypes and of population-based probability maps. Both methods have limitations. Caution has to be urged when gyral variations are taken as MR visible indicators of individual variation in physiology and behavior. However, anatomic variation as depicted in the probability maps may reflect in part inadequacies of the transformation procedure to compensate for all types of individual variation that arise. Given that exact and precise measurements of architectonic parcellation cannot be made in living subjects, we provide information about just how much imprecision is involved when either macroanatomy or classical brain templates are used as a surrogate for cytoarchitecture.

Description of the macroanatomic landmarks is further complicated by the irregular geometry of the temporal transverse gyri which were first studied systematically by Heschl (1878). *In vivo* MR studies report striking intra- and interindividual gyral and sulcal variations which may confound the analysis of structural and functional relationships (Penhune *et al.,* 1996; Leonard *et al.,* 1998). Our postmortem data con-

firm these observations and do not support the hypothesis that a standard anatomical pattern exists for the superior temporal plane with one transverse gyrus on the left side and two transverse gyri on the right side (Pfeifer, 1920). We identified a single transverse gyrus in more than 80% of the hemispheres and did not find consistent asymmetries. Consequently, the definition of a "standard" asymmetric pattern does not seem to be a useful anatomic convention to study how auditory function maps onto the cerebral cortex.

Von Economo and Horn (1930) were the first to study the association between microanatomically defined PAC and the transverse gyri. In our present series, variability of area Te1 was considerably higher than expected from earlier studies (Rademacher *et al.*, 1993). Individual cytoarchitectonic maps representing the standard mapping approach of cytoarchitectonic studies (von Economo and Horn, 1930; Stensaas *et al.*, 1974; Galaburda *et al.*, 1978; Galaburda and Sanides, 1980; Rademacher *et al.*, 1993; Rajkowska and Goldman-Rakic, 1995) show striking interindividual and interhemispheric differences in the topography of area Te1 (Figs. 2 and 3). Area Te1 comprises between 16 and 92% of the cortical volume of HG (Table 2) with no significant correlation between the respective volumes of HG and area Te1. Thus, the extent of area Te1 is grossly overestimated by any approach that interprets HG as the structural equivalent of PAC. When the volume of HG is taken as equal to the size of area Te1, an error of more than 100% is introduced in 22 of 54 (41%) hemispheres (calculated from Table 2). This finding needs to be kept in mind when inferences about the size of PAC are made on the basis of HG volumetry (Penhune *et al.*, 1996).

That a priori information about the microanatomic topography is mandatory has recently been shown for the neuromagnetic approach (Lütkenhöner and Steinsträter, 1998). On one hand, evidence was given that it is possible to register location differences below 1 mm. On the other hand, the application of different analysis strategies gave rise to a "fogging" effect on the order of several millimeters. Comparable uncertainty about the true relationship between structure and function in the auditory system may arise when frequency-related activation is dichotomized along the medial vs lateral half of HG (Strainer *et al.*, 1997). For example, interpretation of bilateral functional data from brains 2B and 2E (Fig. 2) would have been confounded by the striking asymmetries—in opposed directions—of area Te1 in the mediolateral direction. It is evident that anatomic variations of HG like in brain 2F (Fig. 2) make it impossible to infer the extent of area Te1 from the gyral pattern. However, even the presence of an easily identifiable single HG allows for considerable variations in the topography of area Te1. Only with a large enough atlas-based database could one predict the probability of these patterns and the risk of misalignment in matching procedures.

While individual cytoarchitectonic maps do not provide the parametric data for 3-D mapping procedures with data sets from the same or other modalities, they are advantageous in that they visualize the range of individual variations of micro- and macroanatomy. In contrast, averaged maps suffer from a "blurring" effect in this regard and show only the gyral and sulcal topography of the atlas brain (see Figs. 4 and 5).

Landmark-based anatomic interpretation of auditory activation is valid in those particular cases in which area Te1 coincides with HG. In the majority of brains, however, this can be expected to be considerably inaccurate. The zone of maximal overlap (Figs. 4 and 5; dark red, 100%) is small in all planes, indicating high variability. In our brain mapping study, linear alignment of postmortem hemispheres and area Te1 to the standard reference brain reduced interindividual variations in location and extent of area Te1 by reducing the variability in size and spatial position of the brain (Schormann *et al.*, 1997; Schormann and Zilles, 1998). Probabilistic maps have been generated (Figs. 4 and 5) and can be used to localize a region of interest within PAC for a given range of probability. We have shown that this atlas tool permits one to identify retrospectively significant primary auditory activation foci from functional studies within a distinct probability range of area Te1. The probability maps also show that we have to expect considerable variations in the auditory region. The generation of 3-D stereotaxic data sets has permitted us to integrate individual brains and cytoarchitectonic areas into the Talairach coordinate system. Collecting such data for the auditory cortex may be clinically useful for the planning of surgery in patients with intractable temporal lobe epilepsy. The definition of secure borders for anterior temporal lobectomies may be facilitated by the complementary use of probability maps including cytoarchitectonic data.

How closely did the probability map for area Te1 match the location of PAC as identified by the localization of HG in the stereotaxic reference frame of the Talairach atlas? The average location of area Te1 in the present study differs in all dimensions from the location of PAC as defined by HG in previous studies (Penhune *et al.*, 1996; Talairach and Tournoux, 1988). The most striking differences were observed in the mediolateral and anterior–posterior directions. The lateral border of area Te1 is bilaterally located more medially. Right-sided area Te1, which was assumed to be the mirror equivalent of the left-sided area Te1 by Talairach and Tournoux (1988), is located more rostrally. In the axial plane, there were rather small shifts of the superior and inferior borders. The highest degree of mismatch between the stereotaxic coordinates of area Te1 in individual hemispheres and HG in the

Talairach atlas ranged from 14 mm in the axial plane to 18 mm in the coronal plane. This is not surprising, since the location of macroanatomically defined HG in a single hemisphere (Talairach atlas) cannot sufficiently represent the range of intersubject and interhemispheric variability in the population. Topographical uncertainty on the order of centimeters is relevant, because functional studies have indicated that distinct auditory foci may be located only a few millimeters apart. For example, the auditory peak N1m arises from a source located about 5 mm posterior to the middle-latency peak Pam (Pantev *et al.*, 1995).

In contrast to the large number of reports on macroanatomic (Geschwind and Levitsky, 1968; Witelson and Pallie, 1973; Wada *et al.*, 1975; Galaburda *et al.*, 1987; Steinmetz *et al.*, 1989, 1990b; Ide *et al.*, 1996) and architectonic (von Economo and Horn, 1930; Braak, 1978; Galaburda *et al.*, 1978; Witelson *et al.*, 1995) asymmetries in the size of auditory association cortex, such asymmetries have only rarely been studied in PAC (von Economo and Horn, 1930; Rademacher *et al.*, 1993; Penhune *et al.*, 1996; Leonard *et al.*, 1998). In the present study, interhemispheric differences were observed for the location of area Te1 in all dimensions (Table 1). Compared to the left side, right-sided area Te1 is shifted more anterolaterally. Maximum individual asymmetries (i.e., the maximum difference between any pair of hemispheres) of more than 1 cm reflect a topographical asymmetry of the living human brain, because putative methodological factors which may introduce anatomical deformation are generally not expected to influence left–right differences.

Left–right differences in the position of area Te1 imply that there are interhemispheric differences in the location of cortical neurons related to the same auditory process. This asymmetry is relevant for the anatomical interpretation of functional activation in imaging studies. Thus, a task-dependent interhemispheric asymmetry in the center of activation does not necessarily mean that there is a functional lateralization for a given computation involving PAC on one side and association cortex contralaterally. By the same token, identical activation foci may well have their origin from different anatomic modules. Consequently, incongruencies in task-dependent spatial activation patterns may either result from differences in the functional strategy by activating specific but divergent anatomic modules or result from a variant in the bilateral topographical orientation. In a recent functional MR study, there was a lack of cortical activation to a pure tone task in half of the subjects (Strainer *et al.*, 1997). In his commentary, Zatorre (1997) discussed the possibility of differential cognitive processes as a basis for this variability and urged investigators to be cautious in interpreting response differences, unless normative information is available for all task parameters. Given that area Te1 and functionally defined primary auditory foci show similar standard deviations for spatial variability (Dierks *et al.*, 1999), we suggest that it is equally important to control for both functional stimulation parameters and variations in architectonic topography.

Recent MR volume measurements of macroanatomically defined PAC (i.e., combined volumes of HG gray and white matter) revealed significant left > right asymmetries (Penhune *et al.*, 1996). However, segmentation of the volumes in cortical gray and white matter revealed that these asymmetries related only to the white and not the gray matter. In the same study, Penhune *et al.* interpreted their finding of a leftward asymmetry of the white matter beneath HG as a side difference in the volume of cortical fibers that carry information to and from PAC. They suggested that this asymmetry may reflect greater left-sided myelination which could allow faster conduction of nerve impulses and that it may be related to asymmetry of the planum temporale. On the basis of the present architectonic study, we would hesitate to support these speculations because up to 84% of HG are occupied by non-PAC areas (calculated from Table 2). The individual patterns reflect varying proportions of connections to and from primary as well as secondary auditory cortices. Assuming a proportional fiber distribution, one may speculate from our data that—as an average—approximately half of the fiber tracts connect to area Te1. Appropriately designed microanatomic analysis of the auditory radiation may help to define less arbitrary markers of a functionally relevant white matter anatomy. The feasibility of a complementary characterization and spatial mapping of fiber tracts has recently been demonstrated for the human optic radiation (Bürgel *et al.*, 1999).

Our volume measurements of cytoarchitectonically defined PAC demonstrate that there are no significant asymmetries in the size of area Te1. Nevertheless, with a varying degree and direction of asymmetry, more than twofold volume differences may occur between the hemispheres of individual brains. Interhemispheric differences in the number of transverse gyri were not associated with systematic side differences of area Te1. The impressive degree of interhemispheric and interindividual variability makes interpretation of quantitative results from smaller studies difficult. The variability in the volume of area Te1 as estimated by the proportion of the 50% volume (i.e., 50% overlap in the probability map) in relation to the mean volumes (27 brains) is higher than that for Brodmann area 17 (area Te1, ~60% vs area 17, ~70%; lower values indicate higher variability) in a recent cytoarchitectonic study from our laboratory (Amunts *et al.*, 2000). The variability of area 17 is considerably lower than the variability for Brodmann area 18 (~40%) in the same study. It may be speculated that the degree of structural variability follows a hierarchical pattern with

primary cortical regions having smaller variations than the association cortices.

Beyond the macroscopic view, quantitative measures for area Te1 may also help to discuss models of auditory function. Much of our knowledge about the functional organization of the human auditory cortex comes from magnetic source imaging (Romani *et al.*, 1982; Hari, 1990; Hashimoto *et al.*, 1995; Lütkenhöner and Steinsträter, 1998; Ohtomo *et al.*, 1998; Pantev *et al.*, 1998; Salmelin *et al.*, 1998, 1999). Mapping of the sources of the auditory-evoked magnetic fields to the anatomy of the superior temporal plane is of tremendous importance to these studies of brain–behavior relationships. Dependening on which estimate is favored, it has been assumed that to produce the same auditory dipole moment the cortical generator may cover an area of 50 mm^2 (model I (Lütkenhöner and Steinsträter, 1998)) to 1500 mm^2 (model II (Hari, 1990)). With the mean surface area of area Te1 in our sample being ~560 mm^2, model II appears to overestimate the actual dimensions of PAC while model I appears to propose more appropriate numbers.

In conclusion, our data predict that lack of understanding of intra- and interindividual variability of size, shape, and location of area Te1 may lead to structural–functional mismatch of important components of the auditory network. Since variations of both the sulcal pattern and the cytoarchitectonic borders of area Te1 are not significantly correlated, PAC cannot be reliably and precisely localized on high-resolution MR images of the temporal lobe. The probability of localizing area Te1 is higher on the surface of HG compared to the surface of the planum polare or temporale. However, the smaller the distance to the transverse sulci, the greater the probability of finding non-PAC areas. The results provide a rationale for thinking about individual variability and hemispheric asymmetry when designing morphometric and functional studies. Mapping area Te1 to a 3-D human brain has provided a stereotaxic atlas-based tool that can quantify the probability of localizing specific functional properties inside or outside of PAC. The probability maps of a cytoarchitectonic area can be used to clarify the role of variations in both cortical structure and cognitive strategy. We suggest that they represent a more valid approximation to a functionally relevant parcellation system than a gyrus-based reference space.

ACKNOWLEDGMENTS

We are grateful to U. Blohm and C. Opfermann-Rüngeler for their excellent technical assistance. This work was supported by a grant from the Deutsche Forschungsgemeinschaft (SFB 194/A6) and from the Human Brain Project (MH52176P01).

REFERENCES

Amunts, K., Malikovic, A., Mohlberg, H., Schormann, T., and Zilles, K. 2000. Brodmann's areas 17 and 18 brought into stereotaxic space—Where and how variable? *NeuroImage* **11:** 66–84.

Amunts, K., Schleicher, A., Bürgel, U., Mohlberg, H., Uylings, H. B. M., and Zilles, K. 1999. Broca's region revisited: Cytoarchitecture and intersubject variability. *J. Comp. Neurol.* **412:** 319–341.

Braak, H. 1978. On magnopyramidal temporal fields in the human brain—Probable morphological counterparts of Wernicke's sensory speech region. *Anat. Embryol.* **152:** 141–169.

Braak, H. 1980. *Architectonics of the Human Telencephalic Cortex.* Springer-Verlag, Berlin.

Brodmann, K. 1909. *Vergleichende Lokalisationslehre der Grosshirnrinde.* Barth, Leipzig.

Bürgel, U., Schormann, T., Schleicher, A., and Zilles, K. 1999. Mapping of histologically identified long fiber tracts in human cerebral hemispheres to the MRI volume of a reference brain: Position and spatial variability of the optic radiation. *NeuroImage* **10:** 489–499.

Campain, R., and Minckler, J. 1976. A note on the gross configurations of the human auditory cortex. *Brain Lang.* **3:** 318–323.

Clarke, S., and Rivier, F. 1998. Compartments within human primary auditory cortex: Evidence from cytochrome oxidase and acetylcholinesterase staining. *Eur. J. Neurosci.* **10:** 741–745.

Cunningham, D. J. 1892. *Contribution to the Surface Anatomy of the Cerebral Hemispheres.* Royal Irish Acad., Dublin.

Dierks, T., Linden, D. E. J., Jandl, M., Formisano, E., Goebel, R., Lanfermann, H., and Singer, W. 1999. Activation of Heschl's gyrus during auditory hallucinations. *Neuron* **22:** 615–621.

Eberstaller, O. 1890. *Das Stirnhirn. Ein Beitrag zur Anatomie der Oberfläche des Gehirns.* Urban & Schwarzenberg, Vienna/Leipzig.

Galaburda, A., and Sanides, F. 1980. Cytoarchitectonic organization of the human auditory cortex. *J. Comp. Neurol.* **190:** 597–610.

Galaburda, A. M., Corsiglia, J., Rosen, G. D., and Sherman, G. F. 1987. Planum temporale asymmetry: Reappraisal since Geschwind and Levitsky. *Neuropsychologia* **25:** 853–868.

Galaburda, A. M., Sanides, F., and Geschwind, N. 1978. Human brain. Cytoarchitectonic left–right asymmetries in the temporal speech region. *Arch. Neurol.* **35:** 812–817.

Geschwind, N., and Levitsky, W. 1968. Human brain: Left–right asymmetries in temporal speech region. *Science* **161:** 186–187.

Geyer, S., Ledberg, A., Schleicher, A., Kinomura, S., Schormann, T., Bürgel, U., Klingberg, T., Larsson, J., Zilles, K., and Roland, P. E. 1996. Two different areas within the primary motor cortex of man. *Nature* **382:** 805–807.

Geyer, S., Schleicher, A., and Zilles, K. 1999. Areas 3a, 3b, and 1 of human primary somatosensory cortex. *NeuroImage* **10:** 63–83.

Gilbert, A. N., and Wysocki, C. J. 1992. Hand preference and age in United States. *Neuropsychologia* **30:** 601–608.

Hari, R. 1990. The neuromagnetic method in the study of the human auditory cortex. In *Auditory Evoked Magnetic Fields and Electric Potentials. Advances in Audiology* (F. Grandori, M. Hoke, and G. Romani, Eds.). Karger, Basel.

Hashimoto, I., Mashiko, T., Yoshikawa, K., Mizuta, T., Imada, T., and Hayashi, M. 1995. Neuromagnetic measurements of the human primary auditory response. *Electroencephalogr. Clin. Neurophysiol.* **96:** 348–356.

Heschl, R. L. 1878. *Ueber die Vordere Quere Schläfenwindung des Menschlichen Grosshirns.* Wilhelm Braumüller, Vienna.

Hopf, A. 1954. Die Myeloarchitektonik des Isocortex temporalis beim Menschen. *J. Hirnforsch.* **1:** 208–279.

Ide, A., Rodríguez, E., Zaidel, E., and Aboitiz, F. 1996. Bifurcation patterns in the human Sylvian fissure: Hemispheric and sex differences. *Cereb. Cortex* **6:** 717–725.

Lauter, J. L., Herscovitch, P., Formby, C., and Raichle, M. E. 1985. Tonotopic organization in human auditory cortex revealed by positron emission tomography. *Hear. Res.* **20:** 190–205.

Leonard, C., Voeller, K., Lombardino, L., Morris, M., Alexander, A., Andersen, H., Garofalakis, M., Hynd, G., Honeyman, J., Mao, J., Agee, O., and Staab, E. 1993. Anomalous cerebral structure in dyslexia revealed with magnetic resonance imaging. *Arch. Neurol.* **50:** 461–469.

Leonard, C. M., Puranik, C., Kuldau, J. M., and Lombardino, L. J. 1998. Normal variation in the frequency and location of human auditory cortex landmarks. Heschl's gyrus: Where is it? *Cereb. Cortex* **8:** 397–406.

Liegeois-Chauvel, C., Musolino, A., and Chauvel, P. 1991. Localization of primary auditory area in man. *Brain* **107:** 115–131.

Lütkenhöner, B., and Steinsträter, O. 1998. High-precision neuromagnetic study of the functional organization of the human auditory cortex. *Audiol. Neurootol.* **3:** 191–213.

Mazziotta, J. C., Toga, A. W., Evans, A., Fox, P., and Lancaster, J. 1995. A probabilistic atlas of the human brain: Theory and rationale for its development. *NeuroImage* **2:** 89–101.

Merker, B. 1983. Silver staining of cell bodies by means of physical development. *J. Neurosci. Methods* **9:** 235–241.

Ohtomo, S., Nakasato, N., Kanno, A., Hatanaka, K., Shirane, R., Mizoi, K., and Yoshimoto, T. 1998. Hemispheric asymmetry of the auditory evoked N100m response in relation to the crossing point between the central sulcus and Sylvian fissure. *Electroencephalogr. Clin. Neurophysiol.* **108:** 219–225.

Ono, M., Kubik, S., and Abernathey, C. D. 1990. *Atlas of the Cerebral Sulci.* Thieme, Stuttgart/New York.

Pantev, C., Bertrand, O., Eulitz, C., Verkindt, C., Hampson, S., Schuierer, G., and Elbert, T. 1995. Specific tonotopic organizations of different areas of the human auditory cortex revealed by simultaneous magnetic and electric recordings. *Electroencephalogr. Clin. Neurophysiol.* **94:** 26–40.

Pantev, C., Hoke, M., Lehnertz, K., Lütkenhöner, B., Anogianakis, G., and Wittkowski, W. 1988. Tonotopic organization of the human auditory cortex revealed by transient auditory evoked magnetic fields. *Electroencephalogr. Clin. Neurophysiol.* **69:** 160–170.

Pantev, C., Hoke, M., Lehnertz, K., Lütkenhöner, B., Fahrendorf, G., and Stöber, U. 1990. Identification of sources of brain neuronal activity with high spatiotemporal resolution through combination of neuromagnetic source localization (NMSL) and magnetic resonance imaging (MRI). *Electroencephalogr. Clin. Neurophysiol.* **75:** 173–184.

Pantev, C., Oostenveld, R., Engelien, A., Ross, B., Roberts, L. E., and Hoke, M. 1998. Increased auditory cortical representation in musicians. *Nature* **392:** 811–814.

Penhune, V. B., Zatorre, R. J., MacDonald, J. D., and Evans, A. C. 1996. Interhemispheric anatomical differences in human primary auditory cortex: Probabilistic mapping and volume measurement from magnetic resonance scans. *Cereb. Cortex* **6:** 661–672.

Pfeifer, R. A. 1920. Myelogenetisch-anatomische Untersuchungen über das kortikale Ende der Hörleitung. *Abh. Math. Phys. Kl. Sächs. Akad. Wiss.* **37:** 1–54.

Rademacher, J., Caviness, V. S., Jr., Steinmetz, H., and Galaburda, A. M. 1993. Topographical variation of the human primary cortices and its relevance to brain mapping and neuroimaging studies. *Cereb. Cortex* **3:** 313–329.

Rademacher, J., Galaburda, A. M., Kennedy, D. N., Filipek, P. A., and Caviness, V. S., Jr. 1992. Human cerebral cortex: Localization, parcellation, and morphometry with magnetic resonance imaging. *J. Cognit. Neurosci.* **4:** 352–374.

Rajkowska, G., and Goldman-Rakic, P. S. 1995. Cytoarchitectonic definition of prefrontal areas in the normal human cortex. II. Variability in locations of areas 9 and 46 and relationship to the Talairach coordinate system. *Cereb. Cortex* **5:** 323–337.

Rivier, F., and Clarke, S. 1997. Cytochrome oxidase, acetylcholinesterase, and NADPH-diaphorase staining in human supratemporal and insular cortex: Evidence for multiple auditory areas. *NeuroImage* **6:** 288–304.

Roland, P. E., Graufelds, C. J., Wahlin, J., Ingelman, L., Andersson, M., Ledberg, A., Pedersen, J., Akerman, S., Dabringhaus, A., and Zilles, K. 1994. Human brain atlas: For high-resolution functional and anatomical mapping. *Hum. Brain Mapp.* **1:** 173–184.

Romani, G. L., Williamson, S. J., and Kaufman, L. 1982. Tonotopic organization of the human auditory cortex. *Science* **216:** 1339–1340.

Salmelin, R., Schnitzler, A., Parkkonen, L., Biermann, K., Helenius, P., Kiviniemi, K., Kuukka, K., Schmitz, F., and Freund, H. 1999. Native language, gender, and functional organization of the auditory cortex. *Proc. Natl. Acad. Sci. USA* **96:** 10460–10465.

Salmelin, R., Schnitzler, A., Schmitz, F., Jäncke, L., Witte, O. W., and Freund, H.-J. 1998. Functional organization of the auditory cortex is different in stutterers and fluent speakers. *NeuroReport* **9:** 2225–2229.

Sanides, F. 1962. *Die Architektonik des Menschlichen Stirnhirns.* Springer-Verlag, Berlin.

Schlaug, G., Jäncke, L., Huang, Y., and Steinmetz, H. 1995. In vivo evidence of structural brain asymmetry in musicians. *Science* **267:** 699–701.

Schleicher, A., Amunts, K., Geyer, S., Simon, U., Zilles, K., and Roland, P. E. 1999. Observer-independent method for microstructural parcellation of cerebral cortex: A quantitative approach to cytoarchitectonics. *NeuroImage* **9:** 165–177.

Schormann, T., Dabringhaus, A., and Zilles, K. 1997. Extension of the principal axes theory for the determination of affine transformations. In *Proceedings of the DAGM: Informatik-Aktuell,* pp. 384–391. Springer-Verlag, Berlin.

Schormann, T., and Zilles, K. 1998. Three-dimensional linear and nonlinear transformations: An integration of light microscopical and MRI data. *Hum. Brain Mapp.* **6:** 339–347.

Steinmetz, H., Fürst, G., and Freund, H.-J. 1990a. Variation of perisylvian and calcarine anatomic landmarks within stereotaxic proportional coordinates. *Am. J. Neuroradiol.* **11:** 1123–1130.

Steinmetz, H., Rademacher, J., Huang, Y., Hefter, H., Zilles, K., Thron, A., and Freund, H.-J. 1989. Cerebral asymmetry: MR planimetry of the human planum temporale. *J. Comput. Assist. Tomogr.* **13:** 996–1005.

Steinmetz, H., Rademacher, J., Jäncke, L., Huang, Y., Thron, A., and Zilles, K. 1990b. Total surface of temporoparietal intrasylvian cortex: Diverging left–right asymmetries. *Brain Lang.* **39:** 357–372.

Steinmetz, H., Volkmann, J., Jäncke, L., and Freund, H.-J. 1991. Anatomical left–right asymmetry of language-related temporal cortex is different in left- and right-handers. *Ann. Neurol.* **29:** 315–319.

Stensaas, S. S., Eddington, D. K., and Dobelle, W. H. 1974. The topography and variability of the primary visual cortex in man. *J. Neurosurg.* **40:** 747–755.

Strainer, J. C., Ulmer, J. L., Yetkin, F. Z., Haughton, V. M., Daniels, D. L., and Millen, S. J. 1997. Functional MR of the primary auditory cortex: An analysis of pure tone activation and tone discrimination. *Am. J. Neuroradiol.* **18:** 601–610.

Talairach, J., and Tournoux, P. 1988. *A Co-planar Stereotaxic Atlas of the Human Brain.* Thieme, Stuttgart.

von Economo, C., and Horn, L. 1930. Über Windungsrelief, Maße und Rindenarchitektonik der Supratemporalfläche, ihre individuellen und ihre Seitenunterschiede. *Z. Neurol. Psychiat.* **130:** 678–757.

von Economo, C., and Koskinas, G. N. 1925. *Die Cytoarchitektonik der Hirnrinde des Erwachsenen Menschen.* Springer-Verlag, Berlin.

Wada, J. A., Clarke, R., and Hamm, A. 1975. Cerebral hemispheric asymmetry in humans. Cortical speech zones in 100 adult and 100 infant brains. *Arch. Neurol.* **32:** 239–246.

Witelson, S. F., Glezer, I. I., and Kigar, D. L. 1995. Women have greater density of neurons in posterior temporal cortex. *J. Neurosci.* **15:** 3418–3428.

Witelson, S. F., and Kigar, D. L. 1988. Asymmetry in brain function follows asymmetry in anatomical form: Gross, microscopic, postmortem and imaging studies. In *Handbook of Neuropsychology* (F. Boller, J. Grafman, G. Rizzolatti, and H. Goodglass, Eds.). Elsevier, New York.

Witelson, S. F., and Pallie, W. 1973. Left hemisphere specialization for language in the newborn. Neuroanatomical evidence of asymmetry. *Brain* **96:** 641–646.

Zatorre, R. J. 1997. Functional neuroimaging in the study of the human auditory cortex. *Am. J. Neuroradiol.* **18:** 621–623.

Zilles, K., Schlaug, G., Matelli, M., Luppino, G., Schleicher, A., Qü, M., Dabringhaus, A., Seitz, R., and Roland, P. E. 1995. Mapping of human and macaque sensorimotor areas by integrating architectonic, transmitter receptor, MRI and PET data. *J. Anat.* **187:** 515–537.

Zouridakis, G., Simos, P. G., and Papanicolaou, A. C. 1998. Multiple bilaterally asymmetric cortical sources account for the auditory N1m component. *Brain Topogr.* **10:** 183–189.